Dual mechanism controls asymmetric spindle position in ascidian germ cell precursors

F. Prodon, J. Chenevert, C. Hebras, R. Dumollard, E. Faure, J. Gonzalez-Garcia, H. Nishida, C. Sardet, A. Mcdougall

Development 137, 2011-2021 (2010) doi:10.1242/dev.047845

Dual mechanism controls asymmetric spindle position in ascidian germ cell precursors

François Prodon[1], Janet Chenevert[1], Céline Hébras[1], Rémi Dumollard[1], Emmanuel Faure[2], Jose Gonzalez-Garcia[3], Hiroki Nishida[4], Christian Sardet[1] and Alex McDougall[1,*]

SUMMARY

Mitotic spindle orientation with respect to cortical polarity cues generates molecularly distinct daughter cells during asymmetric cell division (ACD). However, during ACD it remains unknown how the orientation of the mitotic spindle is regulated by cortical polarity cues until furrowing begins. In ascidians, the cortical centrosome-attracting body (CAB) generates three successive unequal cleavages and the asymmetric segregation of 40 localized *postplasmic/PEM* RNAs in germ cell precursors from the 8-64 cell stage. By combining fast 4D confocal fluorescence imaging with gene-silencing and classical blastomere isolation experiments, we show that spindle repositioning mechanisms are active from prometaphase until anaphase, when furrowing is initiated in B5.2 cells. We show that the vegetal-most spindle pole/centrosome is attracted towards the CAB during prometaphase, causing the spindle to position asymmetrically near the cortex. Next, during anaphase, the opposite spindle pole/centrosome is attracted towards the border with neighbouring B5.1 blastomeres, causing the spindle to rotate (10°/minute) and migrate (3 μm/minute). Dynamic 4D fluorescence imaging of filamentous actin and plasma membrane shows that precise orientation of the cleavage furrow is determined by this second phase of rotational spindle displacement. Furthermore, in pairs of isolated B5.2 blastomeres, the second phase of rotational spindle displacement was lost. Finally, knockdown of PEM1, a protein localized in the CAB and required for unequal cleavage in B5.2 cells, completely randomizes spindle orientation. Together these data show that two separate mechanisms active during mitosis are responsible for spindle positioning, leading to precise orientation of the cleavage furrow during ACD in the cells that give rise to the germ lineage in ascidians.

KEY WORDS: Asymmetric cell division, Unequal cleavage, Ascidian, Embryo, CAB, Spindle, Mitosis

INTRODUCTION

Asymmetric cell division (ACD) is a means of generating molecularly distinct daughter cells. Mitotic spindles normally orient along the long axis of the cell, dividing the cell into two equal daughters (Hertwig, 1893; Strauss et al., 2006) (for a review, see Galli and Van den Heuvel, 2008). However, during ACD mitotic spindles orient relative to cortical cues (formed through extrinsic or intrinsic means), generating cells that have different size and/or fate (for a review, see Siller and Doe, 2009). ACD is involved in a diverse set of biological processes, ranging from the maintenance of stem cell pool size to the formation of tiny polar bodies in eggs as well as the segregation of cell fate determinants during embryogenesis. During ACD it is important to maintain asymmetric spindle position until the cell division axis is established, which in animal cells occurs during anaphase (for a review, see Von Dassow, 2009).

Many overlapping mechanism organize spindle orientation before and up to the time of cytokinesis. For example, centrosomes align during late interphase/early prophase as a result of the asymmetric distribution of cortical polarity cues. In *Caenorhabditis elegans* one-cell embryos, the centrosome pair is positioned along the anteroposterior axis during interphase owing to astral pulling forces generated by dynein/dynactin complexes (Grill et al., 2001; Gonzy et al., 1999; Couwenbergs et al., 2000). These astral pulling forces interact with asymmetric cortical polarity cues that direct the anteroposterior alignment of the centrosome during interphase. Similarly, in *Drosophila* larval neuroblasts, centrosomes become oriented during late interphase/early prophase (Savoian and Rieder, 2002; Siller et al., 2006; Siller and Doe, 2008). It is interesting to note that despite spindle rocking movements in these cells during mitosis, the spindle remains fixed in the orientation that was defined previously during late interphase/early prophase (Siller et al., 2006; Rusan and Peifer, 2007; Rebollo et al., 2007; Siller and Doe, 2008). One example of spindle reorientation that occurs during mitosis comes from *Drosophila* embryonic neuroblasts, in which the spindle rotates through 90° during prometaphase (Kaltschmidt et al., 2000). However, with the exception of one-cell *C. elegans* embryos, in which spindle displacement towards the posterior pole is induced by activation of the anaphase promoting complex (McCarthy et al., 2009), it is not clear how the cell cycle regulates the position and orientation of the mitotic spindle up to the time of cytokinesis in multicellular animals.

Additional mechanisms can also control spindle orientation. During the four-cell stage in *C. elegans* embryos, the centrosomes in the EMS cell rotate (Hyman and White, 1987) (for a review, see Galli and Van den Heuvel, 2008), owing to signalling between P2 and EMS. This rotational alignment relies on redundant Wnt and Src signalling pathways from P2 to EMS blastomeres, which cause an accumulation of dynactin between P2 and EMS (Zhang et al., 2007). Gα is required for rotational spindle alignment in EMS and may activate dynactin (Zhang et al., 2007). In addition to this cell-cell signalling system, an intrinsic mechanism operates in P2 to

[1]Developmental Biology Unit UMR 7009, UPMC (University of Paris 06) and Centre National de la Recherche (CNRS), Observatoire Océanologique, 06230 Villefranche-sur-Mer, France. [2]ISCPIF-CREA, Ecole Polytechnique–CNRS, 75015 Paris, France. [3]Department of Obstetrics and Gynaecology, School of Medicine, Cardiff University, Heath Park, Cardiff CF14 4XN, UK. [4]Department of Biological Sciences, Graduate School of Science, Osaka University, Toyonaka, Osaka 560-0043, Japan.

*Author for correspondence (alex.mc-dougall@obs-vlfr.fr)

Accepted 8 April 2010

orient the mitotic spindle (as well as P1). Here actin and actin-binding protein accumulate at a cortical site in P1 and P2 during late prophase, and the centrosome is attracted to that site (Waddle et al., 1994). Again, it is not clear how these mechanisms are coordinated with cell cycle progression.

In ascidian embryos a stereotypical pattern of cell division is produced by precisely orienting the plane of cytokinesis in each blastomere up to the 110-cell stage (Conklin, 1905; Hotta et al., 2007). This is most dramatic in the posterior pair of cells that undergo three successive rounds of ACD (from 8–64 cell stage) generating daughter cells of different fate and size. Here a macroscopic structure visible by light microscopy, termed the centrosome-attracting body (CAB), is required for each of these unequal cleavages, generating two small posterior cells that give rise to the germ lineage (Nishikata et al., 1999). About 40 maternal *postplasmic*/*PEM* RNAs accumulate in the CAB, including at least two determinants, *Macho1* and *Pem1* (Yamada, 2006; Prodon et al., 2007; Paix et al., 2009), as well as the germ-cell marker *Vasa* (Fujimura and Takamura, 2000; Paix et al., 2009). The CAB also accumulates a submembranous layer of cortical polarity proteins PAR3, PAR6 and aPKC (Patalano et al., 2006), which are known to be involved in spindle orientation in *C. elegans* one-cell embryos, *Drosophila* neuroblasts and mammalian epithelial cells (for a review, see Siller and Doe, 2009). Classic micromanipulation experiments demonstrated that removal of the CAB abolished ACD and that transplantation of the CAB caused unequal cleavage at an ectopic site (Nishida, 1994; Nishida, 1996; Nishikata et al., 1999). In ascidians it has been postulated that the CAB captures the plus ends of microtubules emanating from one centrosome during interphase (Hibino et al., 1998). This correlates with the observed migration of the nucleus towards the CAB, which depends on microtubules (Nishikata et al., 1999). Maternal *Pem1* (Posterior end mark) mRNA and its protein are localized to the CAB (Negishi et al., 2007). PEM1 is a novel protein that has no known domains. Following knockdown of PEM1, formation of the microtubule bundle linking the centrosome and the posterior cortex does not occur, and the posterior shift of the interphase nuclei is abolished (Negishi et al., 2007). However, as it is the position of the spindle during the metaphase-anaphase transition and not the position of both centrosomes at prophase that determines the orientation of the cleavage plane in animal cells (for a review, see Von Dassow, 2009), it is important to determine precisely how spindle orientation evolves with time up until the point that the cytokinetic furrow is formed.

Even though the relatively enormous size of the ascidian CAB [circa 10-15 μm in *Phallusia* (Patalano et al., 2006)] makes it an excellent system in which to study how a cortical structure regulates microtubule dynamics over three successive cell cycles, it has not been easy to study microtubular dynamics in ascidians. Unfertilized eggs of *Ciona* and *Halocynthia* do not translate exogenous mRNA efficiently (Roure et al., 2007) (see Fig. S1 in the supplementary material). Mainly because of this problem (although opacity and autofluorescence are also factors), few live cell-imaging studies have been performed to follow fluorescent fusion protein dynamics during early cleavage stages in ascidian embryos (Negishi et al., 2007). Before fertilization, the transparent eggs of the ascidian *Phallusia mammillata* translate exogenous mRNA well (see Figs S1 and S2 in the supplementary material), so we combined fast 4D confocal imaging of fluorescent fusion protein constructs with gene-silencing and classical blastomere isolation experiments to determine how the CAB affects spindle dynamics up to the time of cytokinesis. We report for the first time in ascidian embryos that a dual mechanism is responsible for spindle alignment in B5.2 blastomeres at the 16-cell stage. Specifically, one pole of the mitotic spindle (the cab-spindle pole) is attracted towards the CAB, causing the whole spindle to migrate towards the CAB during prometaphase. Next, the opposite spindle pole (the lateral-spindle pole) aligns towards a specific neighbouring blastomere (B5.1) during anaphase, causing the whole spindle to rotate. In isolated pairs of blastomeres from 16-cell-stage embryos, the cab-spindle pole was still attracted towards the CAB, whereas the lateral-spindle pole did not move, indicating that these two mechanisms are separable. Furthermore, knockdown of Pm-Pem1 completely abolished all movement of the mitotic spindle towards the CAB at the 16-cell stage. Finally, during anaphase once these two phases of spindle alignment had taken place, a highly asymmetric cytokinetic furrow propagated across the cell.

MATERIALS AND METHODS

Origin of the animals

Phallusia mammillata were collected at the Roscoff (Brittany, France) and Sète (Etang de Tau, Mediterranean coast, France). Animal handling was as described previously (McDougall and Sardet, 1995).

Microinjection and imaging

Microinjection was performed as previously described (McDougall and Levasseur, 1998). Briefly, dechorionated oocytes were mounted in glass wedges and injected with mRNA (1-2 μg/μl pipette concentration/2-5% injection volume) using a high-pressure system (Narishige IM300). mRNA-injected oocytes were left for 2-5 hours or overnight before fertilization and imaging of fluorescent fusion protein constructs. Pm-Pem1 morpholino (GGCTGTACTGACCACCATTATAACT, GeneTools) was prepared at a concentration of 1 mM in dH_2O and stored at –80°C. Pm-Pem1 morpholino oligonucleotide (MO) was injected at a pipette concentration of 0.3 to 1 mM (~0.2% egg volume). Similar-sized injections of Pm-Pem1 MO at pipette concentrations 0.1 mM did not have any effect. Control MO injections did not affect development. Unfertilized eggs were sometimes co-injected with MAP7::EGFP mRNA, HH2B::Rfp1 mRNA and Pm-Pem1 MO (0.3 mM pipette concentration) 2-3 hours before fertilization or with Pm-Pem1 MO then CKAR protein 2-3 hours before fertilization. FM4-64 (Molecular Probes) was prepared at a concentration of 10 mg/ml in DMSO and diluted in seawater at 20 μg/ml before use. Epifluorescence imaging was performed as previously described (Levasseur and McDougall, 2000). Confocal microscopy was performed using a Leica SP5 or SP2 fitted with 40×/1.3na objective lens. All live imaging experiments were performed at 18-19°C.

Micromanipulation

All manual micromanipulation experiments were performed on an Olympus IX70 microscope using a 10× objective lens. Embryos at the 16-cell stage that displayed MAP7::EGFP fluorescence were mounted in a wedge as described above. With a microinjection needle and hydraulic micromanipulator, pairs of B5.2 blastomere or solitary B5.2 blastomeres were isolated manually.

Quantitation of spindle rotation in fixed embryos

Fixation of 16 cell stage embryos was carried out in cold methanol (–20°C) containing 50 mM EGTA and immunofluorescence was performed as described (Patalano et al., 2006) using primary antibodies against aPKC (sc216 Santa Cruz Biotechnology) to label the CAB and anti-tubulin DM1A (Sigma) or YL1/2 (AbCam) to label centrosomes. Confocal *z*-stacks of images were acquired using a Leica SP2 microscope at intervals of 1-2 μm. The images were rotated for posterior views and the angles measured using 3D projection function in Image J software. Fixation and tubulin labelling of *Halocynthia roretzi* embryos was as described (Nishikata et al., 1999).

Synthesis of RNAs and proteins

We used the Gateway system (Invitrogen) to prepare N- and C-terminal fusion constructs using pSPE3::Venus (a gift from P. Lemaire) and pSPE3::Rfp1 as well as pRN3::EGFP (PH::EGFP) and pRN3::Venus (ABD::Venus). We made the following constructs: Histone H2B::Rfp1 (HH2B was a gift from Z. Polanski, from mouse lung tumour–BI105582), MAP7::EGFP (mouse MAP7 N terminal fragment–BC052637), PH::EGFP (a gift from T. Meyer, encoding the PIP_2 binding domain from human PLCδ1), ABD::Venus [a gift from E. Houliston, based on Pang et al. (Pang et al., 1998)] and also EGFP (from Clontech) cloned in pCS2 and in pSPE3. All synthetic mRNAs were transcribed and capped with mMessage mMachine kit (Ambion).

C kinase activity reporter (CKAR) in the $pRSET_B$ vector (Addgene) was transformed into BL21 *Escherichia coli* (Invitrogen) and CKAR-Histag expression was autoinduced. Fusion protein was then extracted from pelleted bacteria by French press and purified by nickel affinity chromatography (Qiagen), as described previously (Miyawaki and Tsien, 2000). Protein yield was estimated by CFP absorption at 434 nm and 2 mg/ml was used for microinjection.

Image computational processing

Multi-dimensional data were treated, analysed and visualized with Matlab sotfware (MathWorks).

Detection of centrosomes/spindle poles

After a *z*-projection of each *z*-stack, pixels of highest intensity corresponding to the centrosomal signal were detected manually. Next, an automatic correction was applied in order to detect more precisely these pixels of interests: a small region of interest (ROI) (10 pixels*10 pixels*3 slides) was focused on each manually pre-annotated pixel, then a Gaussian filter was applied on these ROIs and spatial coordinates corresponding to the pixels with highest intensity were automatically selected and defined as being the centre of centrosomes.

Spindle pole tracking

In addition to this manual method of centrosome identification, we used the nearest neighbour method to identify centrosomes (this algorithm was appropriate, because centrosomes were well separated between time intervals).

Calculation

Angular speed (ω) corresponds to the difference of angle (dθ) between two segments at two consecutive time steps divided by (dt). Thus ω was determined by the formula {arcos[dot(S1, S2)]/dt}. Linear speed (v) was determined as following: (1) the middle of each spindle was calculated at each time step; (2) then (v) was found by dividing the distance between two consecutive middles (M) with the time interval (dt) (i.e. v=dM/dt). The relationship between angular and linear speed is: (v)=(S*dθ)/dt or (v)=(S)*(ω).

RESULTS

The mitotic spindle moves towards the CAB

We set out to analyse the dynamics of spindle positioning in relation to the CAB before and during the three successive posterior unequal cleavages. We took advantage of the ascidian *Phallusia mammillata* model, in which we could express fluorescent fusion proteins from injected synthetic mRNAs in unfertilized eggs, which is not possible in *Ciona intestinalis* (see Fig. S1 in the supplementary material). Microtubule dynamics were analysed with MAP7::EGFP in posterior blastomeres at the eight- (B5.2), 16- (B6.3) and 32- (B7.6) cell stage in greater detail and revealed that the closest spindle pole was attracted towards the CAB (Fig. 1A,B, yellow star; see also Movie 1 in the supplementary material) and also that the opposite spindle pole (the lateral-spindle pole, Fig. 1) oriented towards the site of contact with neighbouring cells (Fig. 1A,B, blue star; see also Movie 1 in the supplementary material). Neither the timing nor the placement of the cytokinetic furrow was affected by the fluorescent reporters (Fig. 1C).

Computational analysis of 4D confocal image stacks of 16-cell-stage embryos revealed that there were two phases of spindle movement in B5.2 cells (Fig. 2A). Briefly, two phases of increased linear speed were measurable (both ~3 μm/minute; Fig. 2B). Also one phase of increased angular speed was measurable (Fig. 2C, highlighted area). This was equivalent to the lateral-spindle pole rotational alignment to the site of contact between B5.2 and B5.1 cells, causing the angular speed to increase to around 10°/minute (Fig. 2C; see also Movie 2 in the supplementary material).

Spindle orientation occurs after NEB

Following our dynamic imaging studies, we re-examined fixed embryos labelled for microtubules with higher temporal resolution to determine whether we could find evidence of spindle rotational alignment during mitosis. We also analysed spindle position in 16-cell-stage embryos of *P. mammillata* and *Halocynthia roretzi* (two distantly-related ascidian species) to determine whether spindle positioning in ascidians was conserved. In *P. mammillata* we analysed spindle rotation by examining the positions of centrosomes relative to the CAB in a population of 16-cell-stage embryos fixed at different stages of the cell cycle (Fig. 3). Using confocal *z*-series we measured the angle defined by the line connecting the two centrosomes relative to the midline in posterior views of B5.2 cells (Fig. 3B). For cells in prophase [pre-nuclear envelope breakdown (NEB)], this angle was less than 10° (7.7±1.5°, mean ± s.e.m., n=34) showing that the centrosome initially aligned parallel to the animal-vegetal axis. In prometaphase and metaphase, this angle increased to an average of 48° (48±4.4°, mean ± s.e.m., n=28) as the cab-spindle pole approached the CAB. Finally, the spindle completed its rotation and established a position roughly orthogonal to both the animal-vegetal and anteroposterior axes (n=14). These data support the conclusion from dynamic imaging of live embryos (Figs 1, 2; see Movie 1 in the supplementary material) that in *P. mammillata* spindle alignment occurs after NEB in B5.2 cells.

We also examined much larger fixed embryos of *H. roretzi*, the Japanese ascidian species in which the CAB was originally described (Hibino et al., 1998). In these views (Fig. 3C), the distance separating the spindle poles from the midline of the embryo decreases between NEB (left embryo) and cytokinesis (right embryo), confirming that spindle movement towards the CAB also occurs during mitosis in this distantly related ascidian.

Two phases of spindle pole displacement

At the 16-cell stage, final positioning of the mitotic spindle occurred in two phases, whereby the cab-spindle pole was attracted towards the CAB and the lateral-spindle pole towards a site of contact between B5.2 and B5.1 cells. In order to determine whether CAB or lateral-spindle pole alignment was cell autonomous we performed two types of blastomere isolation experiments coupled with 4D fluorescence imaging of microtubules. We isolated pairs of B5.2 blastomeres to determine whether the migration of the lateral-spindle pole towards B5.1 was dependent on cell-cell contact. We also isolated single B5.2 blastomeres to determine whether the cab-spindle pole would be attracted towards the CAB during prometaphase in a cell-autonomous manner.

Pairs of B5.2 cells were isolated manually from the 16-cell-stage embryos with needles in order to determine whether the absence of cell-cell contact between B5.2 and B5.1 would influence the

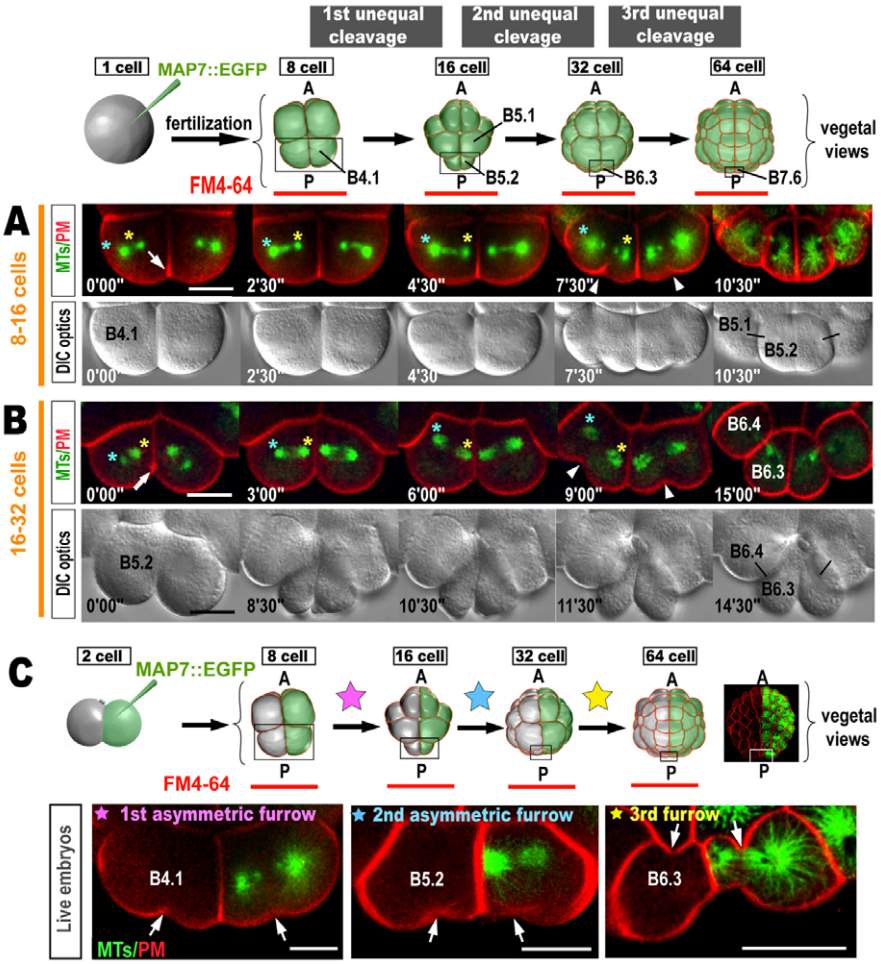

Fig. 1. Spindle orientation from the 8- to 64-cell stage in *P. mammillata*. (**A**) MAP7::EGFP was injected into the unfertilized egg and the embryo bathed in the lipophilic dye FM4-64 as indicated. The first row of images (confocal *z*-projections) display fluorescence from MAP7::EGFP (green) and FM4-64 (red) showing the orientation of the mitotic spindle in two B4.1 blastomeres (posterior view). As the mitotic spindle forms, one pole is attracted towards the edge of the CAB (yellow asterisk, where there is an accumulation of FM4-64, arrow). The opposite spindle pole migrates towards the adjacent cell (blue asterisk). Furrow initiation is indicated by the arrowheads. The differential interference contrast (DIC) images show the relative position of the B5.1 and B5.2 blastomeres and the line on the DIC images shows sister cells. *n*=12. (**B**) At the 16-cell stage one spindle pole (yellow asterisk) again migrates towards the CAB (arrow), after which the opposite spindle pole (blue asterisk) moves towards the neighbouring blastomere. The arrowheads indicate the sites of furrow initiation. *n*=14. (**C**) MAP7::EGFP was injected into one blastomere at the two-cell stage. The embryos were bathed in the lipophilic dye FM4-64 at the times indicated by the red horizontal bars in the diagram. The top row far right image is a vegetal view of a confocal section of the entire embryo at the 64-cell stage [anterior (A) and posterior (P) are indicated]. The lower row of images depicts confocal images of each embryonic stage during cytokinesis, as highlighted on the cartoon by the coloured stars. The white arrows indicate the site of furrow initiation. Note that the timing of furrowing is unaffected by expression of MAP7::EGFP. *n*=15. Scale bars: 40 μm in A; 20 μm in B,C.

alignment of the spindle (Fig. 4A). Three *z*-planes are displayed showing the spindle poles (Fig. 4A). Overlays of planes 1 (green) and 3 (red) display both spindle poles relative to each other. As expected, the cab-spindle pole (green) was attracted towards the CAB during prometaphase (Fig. 4A; see also Movie 3 in the supplementary material). However, migration of the lateral-spindle pole (red) that we observed in the intact embryo (Fig. 1B) did not occur in isolated B5.2 blastomere pairs (see Movie 3 in the supplementary material; *n*=6). Approximately 5-6 minutes after migration of the cab-spindle pole towards the CAB the cell began to divide unequally, forming two small CAB-containing cells (B6.3) (Fig. 4A; see also Movie 5 in the supplementary material).

The CAB attracts the cab-spindle pole during prometaphase in a cell autonomous manner. In solitary B5.2 blastomeres the cab-spindle pole migrated towards the CAB during prometaphase (Fig. 4B and see Movie 4 in the supplementary material). The angle of spindle rotation towards the CAB in isolated B5.2 cells was 38°±8.3 (*n*=8, mean ± s.e.m.). This movement caused unequal cleavage, as one small B6.3 cell was produced (Fig. 4B). As an aside, we also noted that isolated pairs of B5.2 and single B5.2 blastomeres at the 16-cell stage displayed a cortical contraction during interphase, whereby the yolk [labelled with Lysotracker (Molecular Probes; data not shown)] was segregated towards one side of the blastomere (see Fig. 4A,B; see also Movie 4 in the supplementary material).

We next addressed whether the orientation of the lateral spindle pole towards the site of cell-cell contact was the result of B5.2 cell shape, cell signalling from B5.1 to B5.2 or was cell autonomous. As noted above, we found that we could prevent the lateral-spindle pole moving towards the site of cell-cell contact by disrupting the

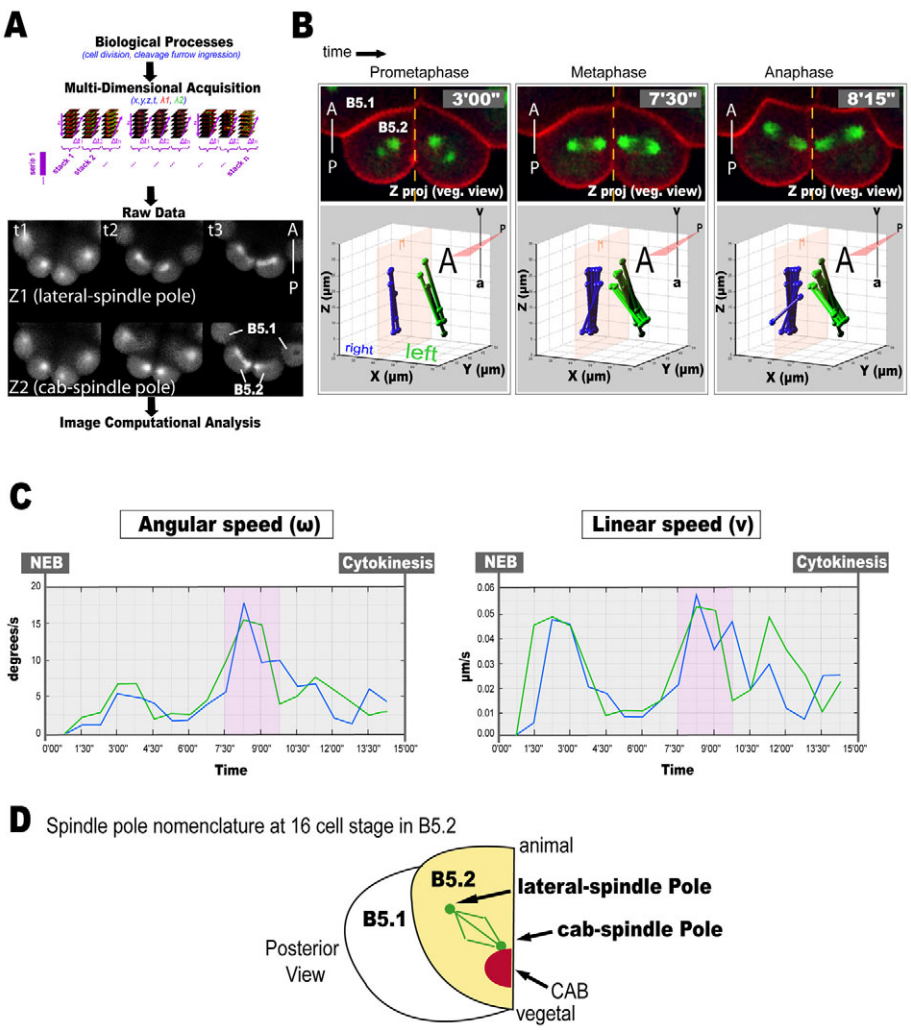

Fig. 2. Computer simulation of spindle-pole movements. (**A**) Experimental design and data analysis. (**B**) Four-dimensional analysis of spindle movement. Top: *z*-projections of four slices extracted from three different stacks acquired 3′00″, 7′30″, 8′15″ after NEB. Orange broken line corresponds to the midline. MTs are in green (MAP7::EGFP) and the PM (FM4-64) in red. Bottom: 3D diagrams made from whole stacks. Spatial coordinates corresponding to the length of spindles (segments) and the position of spindle poles (spheres at the extremities of each segment) were plotted over time in a 3D diagram (*x*, *y*, *z* axis, unit: µm). Left spindle is represented by the green segment and spheres and right spindle by the blue segment and spheres. Position of the spindle at different time steps are superimposed to clearly display the rotation of the spindle. Anterior (A), Posterior (P), animal (a) and vegetal (v) are indicated. (**C**) Graphs showing respectively the angular speed (ω, in degrees/second) and linear speed (v, in µm/second). Blue curves correspond to the spindle in the right (B5.2) blastomere and green curves to the spindle in the left (B5.2). The red highlighted area represents migration of the cab-spindle pole. (**D**) A posterior view of B5.2 (yellow) with spindle (green) and CAB (red) at the 16 cell stage. Animal is up and vegetal down. The cab-spindle pole/centrosome is attracted towards the CAB while the lateral-spindle pole/centrosome migrates the border between B5.2 and B5.1.

contact between B5.1 and B5.2 (Fig. 4; see also Fig. S4B in the supplementary material). However, this also altered B5.2 cell shape (see Fig. S4B in the supplementary material). In order to determine whether cell shape was involved, we were fortunate to observe lateral-spindle pole rotational alignment in two B5.2 cells that had completely different shapes because of slight asynchrony in the adjoining B5.1 cells (see Fig. S4A in the supplementary material). The red stars show the location of the lateral spindle poles in each B5.2 cell before movement towards B5.1 (left column) and 90 seconds later once the movement towards B5.1 had occurred (right). Note that in both B5.2 cells each spindle moves towards the site of cell contact with B5.1 at the same time ±90 seconds (red stars), even though the shape of each B5.2 cell is completely different (see Fig. S4A in the supplementary material). As well as indicating that cell shape was not involved, these data hinted at the possibility that cell signalling was not involved either in the movement of the lateral-spindle pole towards the site of cell-cell contact. To test whether cell signalling was involved we re-associated isolated B5.2 blastomeres with B5.1 and other blastomeres to determine whether we could cause the spindle to rotate towards the site of cell-cell contact. First, re-association of B5.2 with B5.1 did not cause the spindle to rotate towards the site of cell-cell contact (see Fig. S4C in the supplementary material; *n*=11). In these experiments the lateral-spindle pole behaved as though B5.1 was not present [compare with the adjacent image in an embryo where just one B5.1 blastomere is ablated (see Fig. S4B in the supplementary material)]. Other blastomeres were also ineffective in causing the spindle to rotate (data not shown). We therefore suspect that neither cell shape nor signalling are involved and instead conclude that alignment of the lateral-spindle pole towards the site of cell-cell contact probably relies on a cell contact-based mechanism that is disrupted when blastomeres are isolated.

Overall, these blastomere isolation experiments using 16-cell-stage embryos clearly indicate that during prometaphase the CAB functions in a cell-autonomous manner to attract the cab-spindle pole and also that the anterior shift of the lateral-spindle pole requires cell-cell contact.

Pem1 is required for cab-spindle pole migration

In order to further explore the mechanism of spindle orientation in ascidian embryos, we performed knockdown of Pem1. Pem1 protein had previously been shown to be localized to the CAB and to be required for unequal cleavage in CAB-containing cells (Negishi et al., 2007). Knockdown of *P. mammillata* Pem1 (Pm-Pem1) abolished unequal cleavage and resulted in embryos with equal-sized blastomeres at the 16-cell stage as previously described in *H. roretzi* (Negishi et al., 2007) (see Fig. S3 in the supplementary material; *n*=38). In control embryos the cab-spindle pole oriented towards the CAB during prometaphase and remained

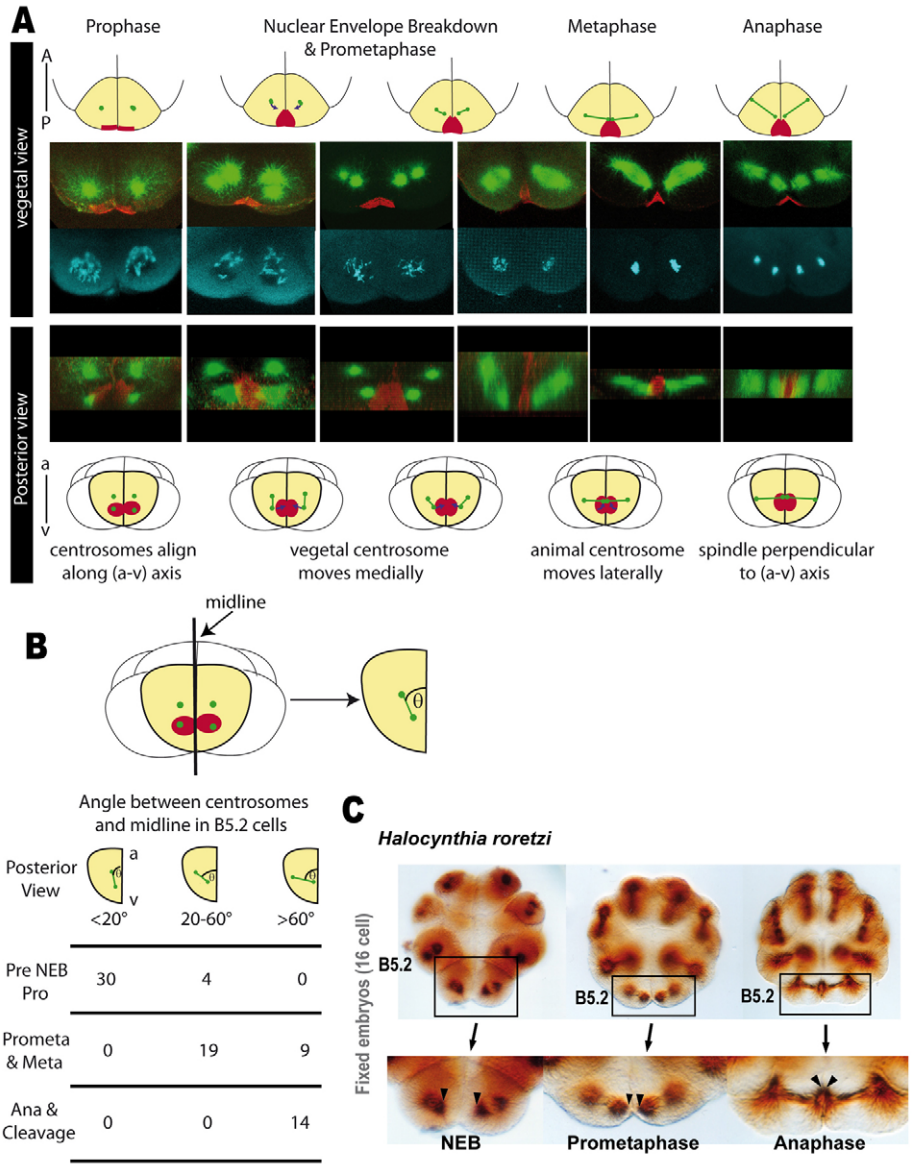

Fig. 3. Spindle position in fixed embryos. (**A**) Confocal images of *P. mammillata* embryos fixed at the 16-cell stage showing microtubules (green, anti-tubulin), CAB (red, anti-aPKC) and DNA (blue, Hoechst). The upper row of images and drawing are a vegetal view, and the lower view was created by rotating the stack 90° to produce a posterior view. Note the alignment of centrosomes parallel to the animal-vegetal axis at prophase (left images) and the perpendicular position of the spindle later (right). The animal-vegetal axis is displayed on the posterior view of the first drawing (a-v). (**B**) The rotation of the spindle was quantified by measuring the angle θ between the centrosomes and the midline for 34 cells in prophase, 28 cells post-NEB and 14 cells in anaphase. The a-v axis is displayed. (**C**) Immunolabelling of microtubules in *H. roretzi* 16-cell stage embryos during three stages of the cell cycle showing that the cab-spindle poles approach the midline after NEB. The lower images display higher magnification of the B5.2 CAB-containing cells. Note that the cab-spindle poles (arrowheads) in each B5.2 cell approach the midline at prometaphase and anaphase.

tethered near the CAB while the lateral-spindle pole migrated towards the neighbouring B5.1 blastomere (Fig. 5A). When viewed from the vegetal side, the spindles in control cells orient to form a characteristic V shape across the midline with cab-spindle poles tethered near the midline (Fig. 5A; see also Movie 6 in the supplementary material). In the absence of Pm-Pem1, the mitotic spindle formed normally and chromosomes congressed during prometaphase, but the spindle failed to move towards the CAB and cells divided obliquely (Fig. 5B; see also Movie 7 in the supplementary material). In the absence of Pm-Pem1 protein, the spindle in both B5.2 cells aligned randomly (Fig. 5B, n=7) and the division plane was not symmetrical across the midline (n=31). In order to follow the position of the CAB with greater accuracy in embryos in which Pm-Pem1 had been knocked down we used C kinase activity reporter (CKAR) protein (n=5). We found fortuitously that this protein labels the CAB (n=12) and does not perturb ACD (see Fig. S5 in the supplementary material). With this probe we could follow the location of the CAB unambiguously and show that the cab-spindle pole does not migrate towards the CAB (see Fig. S5 in the supplementary material, orange stars; n=5) as it does in control embryos (Figs 1, 2 and 3). We also noticed that when eggs were injected with Pem1 MO several hours before fertilization, CKAR localization in embryos became more punctuate and the CAB less compact than in control embryos.

Furrowing is asymmetric in B5.2 blastomeres

We were surprised to find that furrowing was asymmetric in B5.2 blastomeres (Fig. 6A; see also Movie 6 in the supplementary material). Four-dimensional confocal imaging of plasma membrane labelled with PH::EGFP or the lipophilic dye FM4-64 both showed that the furrow started on the outer apical surface and progressed unilaterally towards the inner basolateral surface (Figs 1, 2 and 6; see also Movie 8 in the supplementary material). Filamentous actin (labelled with ABD::Venus) accumulated at the site of active furrowing (Fig. 6Ai; see also Movie 9 in the supplementary material). Asymmetric furrowing in B5.2 blastomeres initiated on the cell surface furthest from the spindle midzone (Fig. 6Aii). We confirmed that furrowing was asymmetric by rotating the data by 90° (Fig. 6Aiii). By performing higher resolution 4D confocal microscopy of MAP7::EGFP in live embryos we could find no

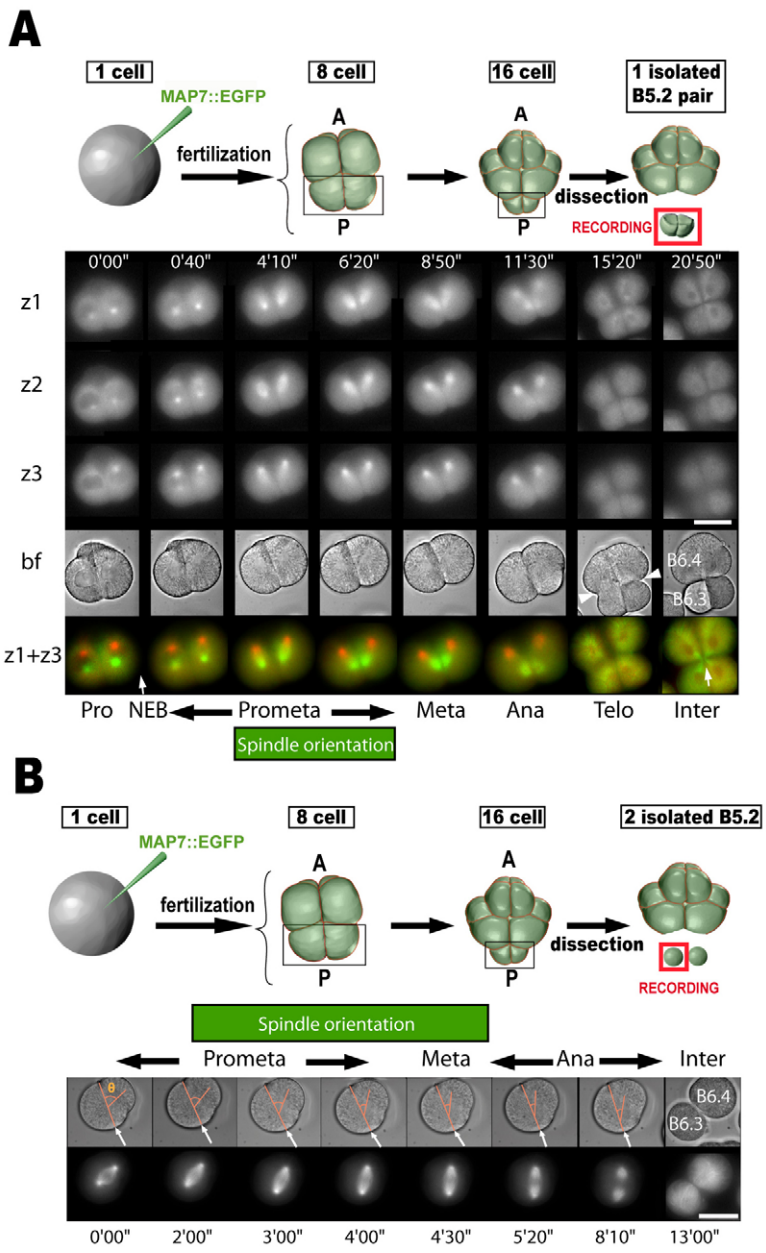

Fig. 4. Spindle position in isolated blastomeres. (**A**) Pairs of B5.2 blastomeres displaying a MAP7::EGFP fluorescence signal were manually dissected from live embryos in natural seawater and subsequently imaged in 4D. Brightfield (bf) image stacks were taken every 10 seconds and fluorescence image stacks every 30 seconds. Three focal planes are displayed (*z*1, *z*2, *z*3). An overlay of *z*1 and *z*3 shows the relative positions of the two spindle poles (*z*1 is green and *z*3 red). One pole (displayed green) was attracted towards the CAB. The opposite spindle pole (red) remained in its original position. The pair of B5.2 blastomeres then underwent unequal cleavage and displayed asymmetric furrowing (arrowheads). Note also that the position of the midbody (20′50″) was close to the midline as a result of asymmetric furrowing (arrow). *n*=7. Also see Movies 3 and 5 in the supplementary material. (**B**) Solitary B5.2 blastomeres were mounted for 4D-fluorescence imaging of MAP7::EGFP. Brightfield image stacks were taken every 10 seconds and fluorescence image stacks every 30 seconds. The mitotic spindle rotated during prometaphase (depicted by angle θ, 38°±8.3°, *n*=8, mean ± s.e.m.) for a period of 2-3 minutes towards the CAB (arrow). Note that at 13′00″ the isolated B5.2 blastomere divided to give one large and one small cell (which contained the CAB, white arrow). *n*=15. Also see Movies 4 and 10 in the supplementary material. Scale bars: 20 µm.

evidence for a decreased density of polymerised microtubules at the site of cell-cell contact (Fig. 6B, circled areas). Also, in the absence of cell-cell contact, furrowing was more symmetric (Fig. 6C, arrowheads; see also Movie 10 in the supplementary material) and the midbody formed centrally (Fig. 6C, arrow), consistent with symmetric furrowing. These data suggest that cell-cell contact in B5.2 hinders furrowing, leading to the unusual situation whereby the cleavage furrow initiates at a site farthest from the spindle midzone and proceeds in a unilateral manner.

DISCUSSION

The ascidian CAB is present from the 8- to the 64-cell stage. It is a large (~15 µm) cortical structure that is present during all phases of the cell cycle and accumulates polarity complex proteins PAR3, PAR6 and aPKC (Patalano et al., 2006), as well as approximately 40 *postplasmic*/*PEM* RNAs (Prodon et al., 2007; Paix et al., 2009). The nucleus and associated centrosomes migrate towards the CAB during interphase (Hibino et al., 1998; Patalano et al., 2006). However, we find that the spindle is also re-positioned following NEB. Using live cell imaging of *P. mammillata* embryos, we demonstrate that one pole of the mitotic spindle migrates towards the CAB during prometaphase in the B4.1/B5.2/B6.3 cells. In-depth analysis of B5.2 blastomeres at the 16-cell stage shows that the vegetal-most spindle pole/centrosome (cab-spindle pole; see Fig. 2D and Fig. 7) is attracted towards the CAB during prometaphase and is then tethered there until furrowing initiates. During anaphase the lateral-spindle pole/centrosome (see Fig. 2D and Fig. 7) is attracted towards the site of cell-cell contact between B5.2 and B5.1. Through a series of blastomere isolation experiments coupled with 4D fluorescence imaging of microtubules and plasma membrane, we demonstrate that displacement of the cab-spindle pole during prometaphase is cell autonomous. Rotational alignment of the lateral-spindle pole requires cell-cell contact.

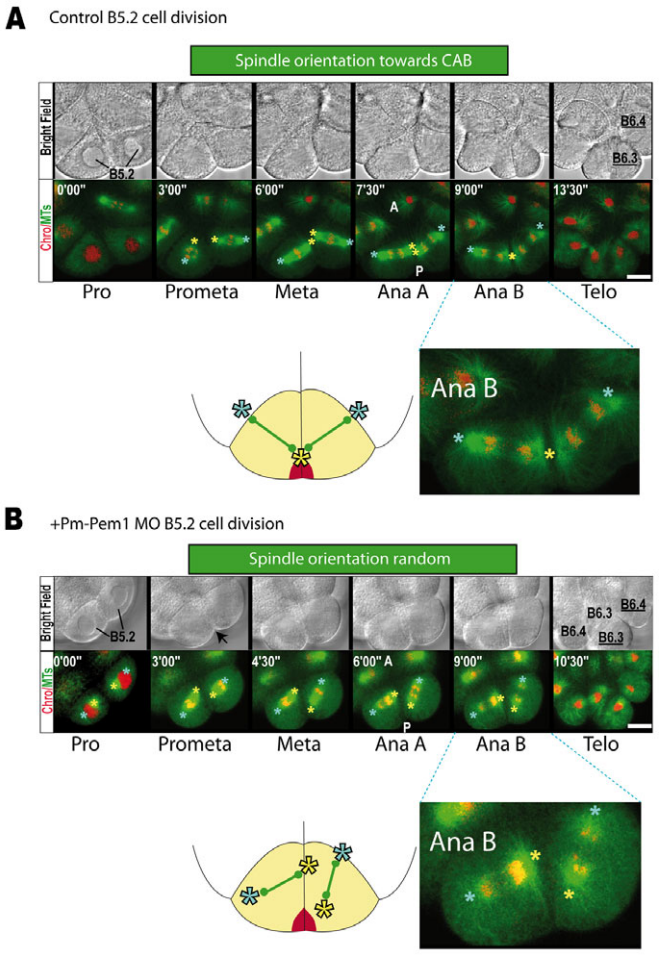

Fig. 5. Pem1 knockdown abolished spindle pole movement towards the CAB. (**A**) Chromosomes are labelled with HH2B::Rfp1 red (Chro) and microtubules with MAP7::EGFP green (MTs). The cab-spindle poles are indicated with yellow asterisks and the lateral spindle poles with blue asterisks. Note that the cab-spindle poles are attracted towards the CAB from prometaphase to anaphase. The lateral-spindle poles migrate towards the adjacent B5.1 blastomere during anaphase A and B. The enlargement and model highlight the orientation of the cab-spindle poles relative to the CAB (red) at Ana B. Also see Movie 6 in the supplementary material. (**B**) Unfertilized eggs were injected with MAP7::EGFP mRNA, HH2B::Rfp1 mRNA and Pm-Pem1 morpholino 2–3 hours before fertilization. Confocal microscopy of spindle alignment during mitosis in Pm-Pem1 MO-injected oocytes. Note that the cab-spindle poles (yellow asterisks) do not align towards each other as they do in A. Instead they align randomly with respect to each other and the CAB. The enlargement and model highlight the random orientation of the cab-spindle poles at Ana B. *n*=7. Also see Movie 7 in the supplementary material. Scale bars: 20 μm.

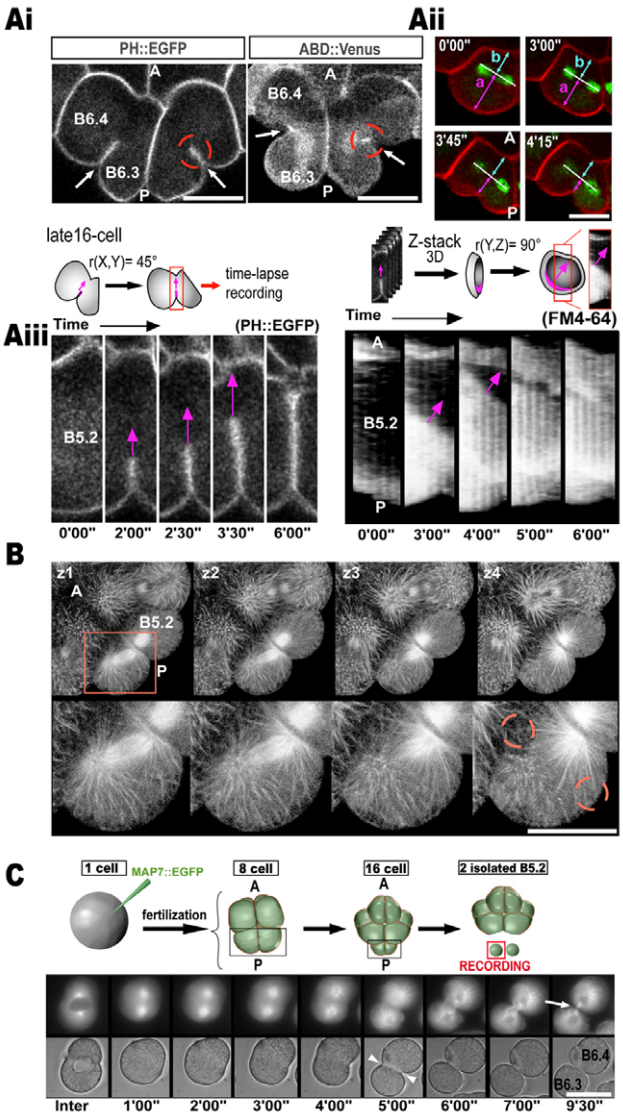

Fig. 6. Asymmetric furrowing and spindle position. The cytokinetic furrow formed asymmetrically in B5.2 blastomeres. (**A**) (i) Confocal image of plasma membrane labelled with PH::EGFP (*n*=12) and filamentous actin with ABD::Venus (*n*=7) in B5.2 during cytokinesis. The arrows and red circle show the progression of the asymmetric furrow. Also see Movies 8 and 9 in the supplementary material. (ii) Confocal image of B5.2 blastomere showing the plasma membrane with FM4-64 (red) and microtubules with MAP7::EGFP (green). Note that the asymmetric furrow initiated at a cortical site far from the position of the spindle (distance a decreases before distance b). *n*=14. (iii) Data from PH::EGFP and FM4-64 was used to visualize the dynamic progression of the asymmetric furrow. The dynamic progression of the asymmetric furrow is displayed then rotated through 90° in order to visualize furrowing from a lateral direction (purple arrows in diagrams above). The anteroposterior axis (A-P) is shown on each image. (**B**) High resolution confocal *z*-section of microtubules labelled with MAP7::EGFP. Four *z*-sections are shown (*z*1-*z*4). The second row of images shows a high resolution zoom of the highlighted area. Note that microtubule bundles approach those parts of the cortex where furrowing occurs (red circled areas). *n*=6. (**C**) MAP7::EGFP fluorescence from widefield images shows how furrowing is symmetric (arrowheads) in B5.2 blastomeres (isolated as shown in diagram above) even though cleavage is still unequal (note smaller B6.3). Also note the central position of the midbody at 9′30″ (arrow) in the top row of images as compared to the asymmetric position in isolated pairs of B5.2 blastomeres (Fig. 4, *z*1+*z*3, 20′50″). *n*=8. Scale bars: 20 μm.

An important question is how spindle orientation is maintained until the cytokinetic furrow is established and cell fate determinants have been segregated. In most documented situations it is the nucleo-centrosome complex (NCC) that re-orients during late interphase/early prophase. This is the case at the 2- to 4- and 4- to 8-cell stages in *C. elegans* embryos (Hyman and White, 1987; Goldstein, 1995) and in *Drosophila* larval neuroblasts (Siller and Doe, 2008). However, as the furrow forms orthogonal to the mitotic spindle (midzone and/or astral microtubules) late during

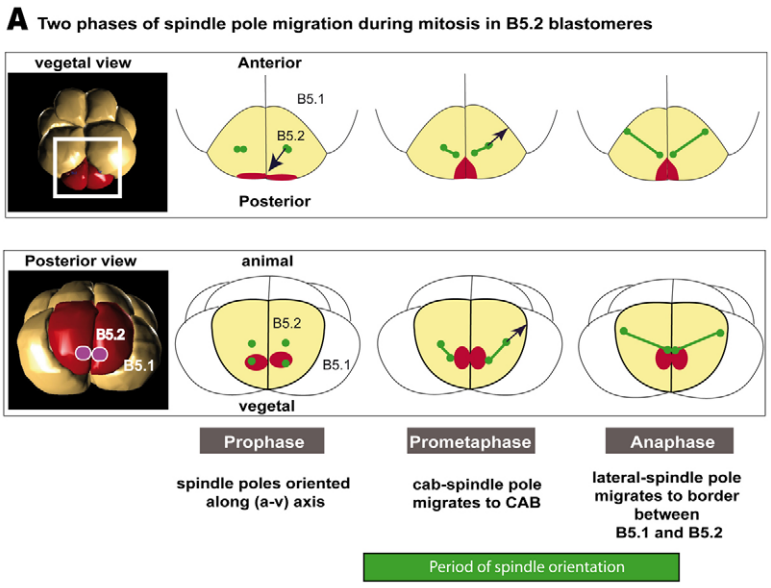

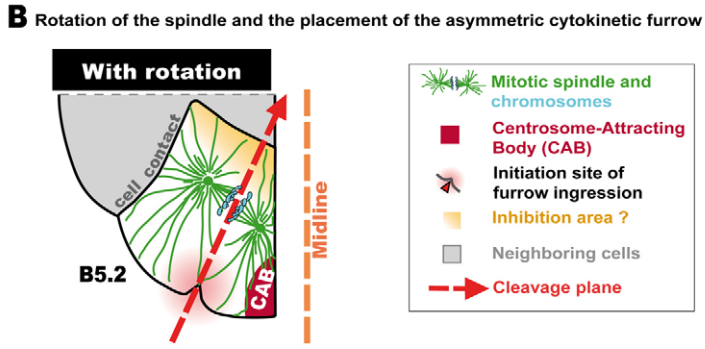

Fig. 7. Model of spindle alignment in B5.2 blastomeres. (**A**) The model depicts the spindle movements in B5.2 that we have observed. The posterior view shows the spindle alignment along the animal-vegetal axis before NEB at the 16-cell stage. Following NEB the vegetalmost centrosome or cab-spindle pole migrates towards the CAB during prometaphase. Later the animalmost centrosome or lateral-spindle pole migrates towards the site of contact with B5.1. Virtual Embryo software (downloaded from http://aniseed-ibdm.univ-mrs.fr/) was used to create the two 3D surface views of 16-cell stage ascidian embryos shown here. (**B**) The final position of the spindle following its rotation is shown relative to the CAB and B5.1 cell before the asymmetric furrow propagates across B5.2, dividing it unequally.

anaphase in animal cells (for a review, see Von Dassow, 2009) (see Movies 6 and 8 in the supplementary material), it is important to maintain spindle orientation until the placement of the furrow is defined. Because the spindle in B5.2 cells is highly mobile, it is clear that placement of the cytokinetic furrow occurs during anaphase in ascidian embryos (see Movies 6 and 8 in the supplementary material). Part of the mechanism that maintains spindle orientation during prometaphase through metaphase has been discovered in *Drosophila* larval neuroblasts. Here Lis1/dynactin is required for spindle rocking movements and orientation of the spindle from prophase to metaphase (Siller and Doe, 2008). However, it is still not known how spindle orientation is maintained after metaphase up until the time of cytokinesis (Siller and Doe, 2008). Yet another piece of the puzzle comes from the finding that in *Drosophila* larval neuroblasts the cell-cycle-regulated kinases Aurora-A (Lee et al., 2006) and Polo (Wang et al., 2007) are also involved in asymmetric spindle orientation. A recent study in *Drosophila* S2 cells revealed that aurora-A phosphorylates a serine residue in the linker region of Pins that triggers Dlg and Khc73 recruitment to Pins and the subsequent spindle-organizing activity of the Pins cortical complex (Johnson et al., 2009). However, this still does not explain how spindle orientation is maintained until cytokinesis is initiated. Some progress has been made in understanding how the mitotic spindle can be displaced during anaphase in *C. elegans*. Here the anaphase-promoting complex/cyclosome (APC/C) is involved in triggering spindle displacement precisely at the time of anaphase onset (McCarthy et al., 2009). The theme emerging from these studies is that mechanisms exist that control the asymmetric position and orientation of the spindle so that the cytokinetic furrow forms in the appropriate place during ACD.

Here we have revealed the mechanism whereby the orientation of the mitotic spindle in ascidians is controlled up to the point of furrowing. We found that the final placement of the mitotic spindle at the 16-cell stage in B5.2 cells in ascidians depends on two independent and separable movements of the whole mitotic spindle. The first movement involves the CAB, which constitutes an intrinsic cortical site that attracts the cab-spindle pole. The lateral-spindle pole is then attracted towards the site of contact between B5.2 and B5.1 cells. These two independent movements precisely orient the whole spindle and the plane of cytokinesis. Part of the mechanism that attracts the spindle to the CAB involves PEM1, which is necessary for unequal cleavage divisions in these posterior cells (Negishi et al., 2007) (for a review, see Munro, 2007). It has previously been reported that in the absence of PEM1, gastrulation occurs but is incomplete and embryos subsequently develop into abnormal larvae lacking an apparent anteroposterior axis (Negishi et al., 2007). We also find that Pm-Pem1 MO disrupts gastrulation and leads to the development of larvae with severely shortened tails (see Fig. S3 in the supplementary material). However, as PEM1 is likely to have functions in addition to spindle orientation, it is not possible to know whether it is these spindle-position independent functions of PEM1 that are required for gastrulation and further development.

Another part of the mechanism that controls spindle alignment involves cell-cell contact between B5.2 and B5.1. We found that this was independent of the shape of B5.2 cells and also cell signalling. We surmise that some form of structure that links B5.1 and B5.2 such as the midbody remnant or junctional complex may be involved in causing the B5.2 spindle to rotate towards B5.1 during anaphase. Such a structure has already been described in two-cell *C. elegans* embryos, in which an actin-rich cortical structure forms in P1 blastomeres around the midbody remnant that attracts one centrosome during late prophase (Waddle et al., 1994). Finally, an important point is whether the first spindle movement towards the CAB is necessary for the second movement to occur. From our Pem1 knockdown experiments we noted that not only was division symmetric but that both spindle poles appeared to orient randomly in the blastomeres. This may indicate that Pem1 is also present on the cortex between B5.2 and B5.1, where it controls positioning of the lateral centrosome/spindle pole, or alternatively that in the absence of a functioning CAB geometrical constraints take precedence over the attractive force that exists between B5.2 and B5.1 so that spindle position is altered.

An unexpected aspect of the asymmetric spindle positioning that we have described here is that it is accompanied by an asymmetric furrow that initiates far from the central spindle (Figs 6, 7). We found that filamentous actin accumulation occurs locally at the site of furrowing, and our cell isolation experiments indicated that furrowing was inhibited by cell-cell contact. It is possible that asymmetric furrowing is more widespread in ascidian blastomeres during cleavage stages. The small GTPase RhoA is the main regulator of actin dynamics during cytokinesis (for a review, see Barr and Gruneberg, 2007). We would therefore predict that there is an unequal distribution of RhoA regulators such as Ect2 or MgcRacGAP on the cortex (for a review, see Barr and Gruneberg, 2007). Another important question is whether there is a link between asymmetric cell division and the asymmetric furrow that we have described. Although we currently do not know what role this asymmetric furrowing may play, it is interesting to note that one consequence is that the midbody forms deep inside the embryo. However, this may have a more general role, as other blastomeres also appear to display asymmetric furrowing (data not shown). In mammalian epithelial cells the midbody is also located on one side of the polarised cell as a result of asymmetric furrowing and plays a role in polarisation of that cell (Fleming et al., 2007; Dubreuil et al., 2007).

In the ascidian embryo, CAB-induced asymmetric spindle positioning in the B4.1/B5.2/B6.3 lineage results in three unequal cleavages that give rise to two small posterior germ-cell precursors that inherit the CAB and more than 40 maternal *postplasmic*/*PEM* RNAs including *Vasa* (Fujimura and Takamura, 2000; Yamada, 2006; Prodon et al., 2007; Paix et al., 2009). We show that in ascidian embryos a dual mechanism precisely positions the cab-spindle pole then the lateral-spindle pole, leading to the precise reorientation of the mitotic spindle in both B5.2 cells before cell division. Recent data have highlighted the importance of the link between the cell cycle machinery and the coordination of ACD (Johnson et al., 2009; McCarthy Campbell et al., 2009). The ascidian will probably provide an interesting model to determine precisely how a cortical microtubule-organizing centre (the CAB) is activated by the cell cycle during prometaphase.

Acknowledgements
We would like to thank the ANR (08-BLAN-0136-02), ARC, AFM and ATIP for financial support. Francois Prodon was supported by an ANR postdoctoral position. We would also like to thank Patrick Chang and Mark Levasseur for helpful comments and Karl Swann for collaborating with CKAR protein.

Competing interests statement
The authors declare no competing financial interests.

Supplementary material
Supplementary material for this article is available at
http://dev.biologists.org/lookup/suppl/doi:10.1242/dev.0047845/-/DC1

References
Barr, F. A. and Gruneberg, U. (2007). Cytokinesis: placing and making the final cut. *Cell* **131**, 847-860.
Brand, A. H. (2008). A new dawn for Aurora. *Nat. Cell Biol.* **10**, 1253-1254.
Conklin, E. G. (1905). The organization and cell lineage of the ascidian egg. *J. Acad. Natl. Sci. Philadelphia* **13**, 1-119.
Couwenbergs, C., Labbé, J. C., Goulding, M., Marty, T., Bowerman, B. and Gotta, M. (2000). Heterodimeric G protein signaling functions with dynein to promote spindle positioning in *C. elegans*. *J. Cell Biol.* **179**, 15-22.
Dubreuil, V., Marzesco, A.-M., Corbeil, D., Huttner, W. B. and Wilsch-Brauninger, M. (2007). Midbody and primary cilium of neural progenitors release extracellular membrane particles enriched in the stem cell marker prominin-1. *J. Cell Biol.* **176**, 483-495.
Fleming, E. S., Zajac, M., Moschenross, D. M., Montrose, D. C., Rosenberg, D. W., Cowan, A. E. and Tirnauer, J. S. (2007). Planar spindle orientation and asymmetric cytokinesis in the mouse small intestine. *J. Histochem. Cytochem.* **55**, 1173-1180.
Fujimura, M. and Takamura, K. (2000). Characterization of an ascidian DEAD-box gene, Ci-DEAD1: specific expression in the germ cells and its mRNA localization in the posterior most blastomeres in early embryos. *Dev. Genes Evol.* **210**, 64-72.
Galli, M. and van den Heuvel, S. (2008). Determination of the cleavage plane in early *C. elegans* embryos. *Annu. Rev. Genet.* **42**, 389-411.
Goldstein, B. (1995). Cell contacts orient some cell division axes in the *Caenorhabditis elegans* embryo. *Development* **129**, 1071-1080.
Gonzy, P., Pichler, S., Kirkham, M. and Hyman, A. A. (1999). A cytoplasmic dynein is required for distinct aspects of MTOC positioning, including centrosome separation, in the one cell stage *Caenorhabditis elegans* embryo. *J. Cell Biol.* **147**, 135-150.
Grill, S. W., Gonczy, P., Stelzer, E. H. and Hyman, A. A. (2001). Polarity controls forces governing asymmetric spindle positioning in *Caenorhabditis elegans* embryo. *Nature* **409**, 630-633.
Hertwig, O. (1893). Ueber den Werth der ersten Furchungszellen fur die Organbildung des Embryo. Experimentelle Studien am Frosch und Tritonei. *Arch. Mikrosk. Anat.* **42**, 662-804.
Hibino, T., Nishikata, T. and Nishida, H. (1998). Centrosome-attracting body: A novel structure closely related to unequal cleavages in the ascidian embryo. *Dev. Growth Differ.* **40**, 85-95.
Hotta, K., Mitsuhara, K., Takahashi, H., Inaba, K., Oka, K., Gojobori, T. and Ikeo, K. (2007). A web-based interactive developmental table for the ascidian *Ciona intestinalis*, including 3D real-image embryo reconstructions: I. From fertilized egg to hatching larva. *Dev. Dyn.* **236**, 1790-1805.
Hyman, A. A. and White, J. (1987). Determination of cell division axes in the early embryogenesis of *Caenorhabditis elegans*. *J. Cell Biol.* **105**, 2123-2135.
Johnson, C. A., Hirono, K., Prehoda, K. E. and Doe, C. Q. (2009). Identification of an Aurora-A/Pins linker/Dlg spindle orientation pathway using induced cell polarity in S2 cells. *Cell* **138**, 1150-1163.
Kaltschmidt, J. A., Davidson, C. M., Brown, N. H. and Brand, A. H. (2000). Rotation and asymmetry of the mitotic spindle directs asymmetric cell division in the developing central nervous system. *Nat. Cell Biol.* **2**, 7-12.
Lee, C. Y., Andersen, R. O., Cabernard, C., Manning, L., Tran, K. D., Lanskey, M. J., Bashirullah, A. and Doe, C. Q. (2006). *Drosophila* Aurora-A kinase inhibits neuroblast self-renewal by regulating aPKC/Numb cortical polarity and spindle orientation. *Genes Dev.* **20**, 3464-3474.
Levasseur, M. and McDougall, A. (2000). Sperm-induced calcium oscillations at fertilisation in ascidians are controlled by cyclin B1-dependent kinase activity. *Development* **127**, 631-641.
McCarthy Campbell, E. K., Werts, A. D. and Goldstein, B. (2009). A cell cycle timer for asymmetric spindle positioning. *PLoS Biol.* **7**, e1000088.
McDougall, A. and Sardet, C. (1995). Functions and characteristics of repetitive calcium waves associated with meiosis. *Curr. Biol.* **3**, 318-328.
McDougall, A. and Levasseur, M. (1998). Sperm-triggered calcium oscillations during meiosis in ascidian oocytes first pause, restart then stop: correlations with cell cycle kinase activity. *Development* **125**, 4451-4459.
Miyawaki, A. and Tsien, R. Y. (2000). Monitoring protein conformations and interactions by fluorescence resonance energy transfer between mutants of green fluorescent protein. *Methods Enzymol.* **327**, 472-500.
Munro, E. (2007). Asymmetric cell division: A CAB driver for spindle movements. *Curr. Biol.***17**, R639-R641.
Negishi, T., Takada, T., Kawai, N. and Nishida, H. (2007). Localized PEM mRNA and protein are involved in cleavage-plane orientation and unequal cell division in ascidians. *Curr. Biol.* **17**, 1014-1025.

Nishida, H. (1994). Localization of determinants for formation of the anterior-posterior axis in eggs of the ascidian *Halocynthia roetzi*. *Development* **120**, 3093-3104.
Nishida, H. (1996). Vegetal egg cytoplasm promotes gastrulation and is responsible for specification of vegetal blastomeres in embryos of the ascidian *Halocynthis roretzi*. *Development* **122**, 1271-1279.
Nishikata, T., Hibino, T. and Nishida, H. (1999). The centrosome-attracting body, microtubule system, and posterior egg cytoplasm are involved in positioning of cleavage planes in the ascidian embryo. *Dev. Biol*. **209**, 72-85.
Paix, A., Yamada, L., Dru, P., Lecordier, H., Pruliere, G., Chenevert, J., Satoh, N. and Sardet, C. (2009). Cortical anchorages and cell type specifications of maternal *postplasmic/PEM* RNAs in ascidians. *Dev. Biol*. **336**, 96-111.
Pang, K. M., Lee, E. and Knecht, D. A. (1998). Use of a fusion protein between GFP and an actin-binding domain to visualize transient filamentous-actin structures. *Curr. Biol.* **8**, 405-408.
Patalano, S., Prulière, G., Prodon, F., Paix, A., Dru, P., Sardet, C. and Chenevert, J. (2006). The aPKC-PAR-6-PAR-3 cell polarity complex localizes to the centrosome-attracting body, a macroscopic cortical structure responsible for asymmetric divisions in the early ascidian embryo. *J. Cell Sci.* **119**, 1592-1603.
Prodon, F., Yamada, L., Shirae-Kurabayashi, M., Nakamura, Y. and Sasakura, Y. (2007). *Postplasmic/PEM* RNAs: a class of localized maternal mRNAs with multiple roles in cell polarity and development in ascidian embryos. *Dev. Dyn.* **236**, 1698-1715.
Rebollo, E., Sampaio, P., Januschke, J., Llamazares, S., Varmark, H. and González, C. (2007). Functionally unequal centrosomes drive spindle orientation in asymmetrically dividing *Drosophila* neural stem cells. *Dev. Cell* **12**, 467-474.
Roure, A., Rothbächer, U., Robin, F., Kalmar, E., Ferone, G., Lamy, C., Missero, C., Mueller, F. and Lemaire, P. (2007). A multicassette Gateway vector set for high throughput and comparative analyses in *Ciona* and vertebrate embryos. *PLoS One* **2**, e916.
Rusan, N. M. and Peifer, M. A. (2007). A role for a novel centrosome cycle in asymmetric cell division. *J. Cell Biol.* **177**, 13-20.
Savoian, M. S. and Rieder, C. L. (2002). Mitosis in primary cultures of *Drosophila melanogaster* larval neuroblasts. *J. Cell Sci*. **115**, 3061-3072.
Siller, K. H. and Doe, C. Q. (2008). Lis1/dynactin regulates metaphase spindle orientation in *Drosophila* neuroblasts. *Dev. Biol*. **319**, 1-9.
Siller, K. H. and Doe, C. Q. (2009). Spindle orientation during asymmetric cell division. *Nat. Cell Biol.* **11**, 365-374.
Siller, K. H., Cabernard, C. and Doe, C. Q. (2006). The NuMA-related Mud protein binds Pins and regulates spindle orientation in *Drosophila* neuroblasts. *Nat. Cell Biol.* **8**, 594-600.
Strauss, B., Adams, R. J. and Papalopulu, N. (2006). A default mechanism of spindle orientation based on cell shape is sufficient to generate cell fate diversity in polarised *Xenopus* blastomeres. *Development* **133**, 3883-3893.
Von Dassow, G. (2009). Concurrent cues for cytokinetic furrow induction in animal cells. *Trends Cell Biol*. **19**, 165-173.
Waddle, J. A., Cooper, J. A. and Waterston, R. H. (1994). Transient localized accumulation of actin in *Caenorhabditis elegans* blastomeres with oriented asymmetric divisions. *Development* **120**, 2317-2328**.**
Wang, H., Ouyang, Y., Somers, W. G., Chia, W. and Lu, B. (2007). Polo inhibits progenitor self-renewal and regulates Numb asymmetry by phosphorylating Pon. *Nature* **449**, 96-100.
Yamada, L. (2006). Embryonic expression profiles and conserved localization mechanisms of pem/postplasmic mRNAs of two species of ascidian, *Ciona intestinalis* and *Ciona savignyi*. *Dev. Biol.* **296**, 524-536.
Zhang, H., Skop, A. R. and White, J. G. (2007). Src and Wnt signaling regulate dynactin accumulation to the P2-EMS cell border in *C. elegans* embryos. *J. Cell Sci.* **121**, 155-161.